Divacancy acceptor levels in ion-irradiated silicon

B. G. Svensson and B. Mohadjeri
The Royal Institute of Technology, Solid State Electronics, P.O. Box 1298, S-164 28 Kista-Stockholm, Sweden

A. Hallén
Department of Radiation Sciences, Uppsala University, P.O. Box 535, S-751 21 Uppsala, Sweden

J. H. Svensson
Department of Physics and Measurement Technology, University of Linköping, S-581 83 Linköping, Sweden

J. W. Corbett
Department of Physics, The State University of New York at Albany, Albany, New York 12222
(Received 7 June 1990)

High-purity n-type silicon samples have been irradiated with mega-electron-volt ions ($^{1}H^{+}$, $^{4}He^{2+}$, $^{16}O^{4+}$, $^{32}S^{7+}$, $^{79}Br^{8+}$, and $^{127}I^{10+}$), and the two divacancy-related acceptor levels ~ 0.23 and ~ 0.42 eV below the conduction band (E_c), respectively, have been studied in detail using deep-level transient spectroscopy (DLTS). Depth concentration profiles show identical values for the two levels at shallow depths, while in the region close to the damage peak large deviations from a one-to-one proportionality are found. These deviations increase with ion dose and also hinge strongly on the density of energy deposited into elastic collisions per incoming ion. Evidence for a model of the two levels is presented and, in particular, the model invokes excited states caused by motional averaging and lattice strain associated with damaged regions. The divacancy center is known to exhibit a pronounced Jahn-Teller distortion at low temperatures (≤ 20 K), and three equivalent electronic distortion directions exist. However, at higher temperatures (≥ 30 K) reorientation (bond switching) from one distortion direction to another takes place; in a perfect lattice the reorientation rate ultimately becomes so high that the defect does not relax in the distorted configurations, and a motionally averaged state with an effective point-group symmetry of D_{3d} appears. At the temperatures where the DLTS peaks at $E_c-0.23$ and $E_c-0.42$ eV are observed, the reorientation time for bond switching is several orders of magnitude smaller than the time for electron emission from the two levels. This implies strongly that the levels originate from the motionally averaged state and not from the distorted state. Consequently, a clear distinction must be made between these DLTS peaks and the charge-state transitions observed in low-temperature studies where the divacancy is frozen in one of the three equivalent distorted configurations. Finally, the association of electronic energy levels with motionally averaged states is expected to apply not only for the divacancy but also for other defects where dynamic effects occur, e.g., the monovacancy and the E center.

I. INTRODUCTION

In 1961 Corbett and Watkins[1] attributed the two electron-spin-resonance spectra Si-$G6$ and Si-$G7$ occurring in electron-irradiated silicon to the divacancy center (V_2). (In the original work the two spectra were labeled Si-J and Si-C, respectively.) The spectra were interpreted as arising from a singly positive and singly negative charge state of V_2, respectively. Furthermore, no resonances were observed in low-resistivity n-type material indicating that V_2 may appear in four different charge states $(+,0,-,2-)$. This has subsequently been confirmed by a variety of different experimental techniques, e.g., electron paramagnetic resonance (EPR),[2] photoconductivity,[3,4] infrared absorption (IR),[5–8] electron-nuclear double resonance,[9,10] and deep-level transient spectroscopy (DLTS),[11,12] although some controversy exists about the exact positions in the forbidden band gap of the different transitions.

The unperturbed configuration of V_2 has a D_{3d} point-group symmetry with the high-symmetry axis along the four equivalent $\langle 111 \rangle$ directions. However, in the charge states $+$, 0, and $-$ degenerate and partially occupied orbitals appear, and a Jahn-Teller distortion takes place which lowers the symmetry to C_{2h}. This has been experimentally confirmed for V_2^{+} and V_2^{-} by EPR measurements performed at low temperatures (≤ 20 K) where the defect is frozen in one of the three equivalent configurations corresponding to the C_{2h} state.[2] At high enough temperatures (≥ 30 K) a thermally activated reorientation (bond switching) between the three equivalent distortion directions is initiated, and the jump rate may become so high that the defect does not relax in the low-symmetry configurations; a motionally averaged state with the effective symmetry of D_{3d} appears, and V_2 becomes a six-silicon-atom center. It is important to emphasize that the motion implies electronic bond switching and not atom motion; this state was first observed by

Watkins and Corbett[2] and subsequently confirmed by Sieverts and co-workers,[9,10] who reported a "surprisingly good" sp^3 bonding of the state with respect to the nearest-neighbor atoms.

On the basis of DLTS studies of the generation rate versus bombardment energy, annealing kinetics, and depth concentration profiles the following level scheme has been proposed;[11,12] $E_v+0.25$ eV: V_2 (0/+; of charge state 0 if the level is occupied by an electron; + if unoccupied); $E_c-0.42$ eV: $V_2(-/0)$; and $E_c-0.23$ eV: $V_2(2-/-)$ where E_v and E_c represent the valence band and the conduction band, respectively. One controversy concerns the large electron capture cross section of the latter level ($\sim 10^{-15}$–10^{-16} cm^2).[11,13] This is about 4 to 5 orders of magnitude higher than expected for a repulsive and highly localized single minus charge site ($\sim 10^{-19}$–10^{-21} cm^2). Interpretations where V_2 is regarded as a highly distorted center have been put forward, and configurational relaxations accompanying the change in charge state have been assumed. The symmetry of V_2^{2-} should be D_{3d} since no Jahn-Teller distortion is present (the e_u level is filled and no splitting is expected). This symmetry has never been confirmed experimentally since no EPR signal is observable for V_2^{2-}, i.e., the two acceptor electrons act as a pair. Moreover, low-temperature EPR measurements (~ 10 K) do not even give any indirect evidence for the existence of the $E_c-0.23$ eV level attributed to V_2^{2-}. In a generation rate versus dose study Sieverts *et al.*[14] observed simultaneously the vacancy-oxygen center (spectrum $B1$) and V_2^- (spectrum $G7$) indicating that there is no V_2-related energy level between the vacancy-oxygen level at $E_c-0.17$ eV and the $G7$ level. Similar conclusions have been made by Svensson *et al.*[8] from low-temperature IR measurements (9 K) showing that the 0.34-eV absorption peak (originating from V_2^-) is present in samples where the Fermi level is above $E_c-0.17$ eV.

For electron-irradiated samples a close one-to-one relationship between the strengths of the levels $E_c-0.23$ eV and $E_c-0.42$ eV has been found in DLTS studies.[11,12] However, recent results for MeV proton- and α-bombarded p^+-n diodes reveal a difference in dose dependence for the two levels, and a linear correlation does not hold for these samples.[15] In this work we have carefully compared the depth profiles of [$E_c-0.23$ eV] and [$E_c-0.42$ eV] (square brackets denote concentration values) in ion-bombarded specimens. The profiles are identical at shallow depths while in the region at maximum damage density [$E_c-0.42$ eV] is significantly larger than [$E_c-0.23$ eV]. The profiles have been investigated as a function of dose and for various types of bombarding ions ($^1H^+$, $^4He^{2+}$, $^{16}O^{4+}$, $^{32}S^{7+}$, $^{79}Br^{8+}$, and $^{127}I^{10+}$). The origin of the two levels is discussed in detail, and evidence for a new model is presented. In particular, the model invokes excited states caused by motional averaging and lattice strain associated with "highly" damaged regions which may prevent electronic bond switching. In the studied temperature range, it is found that the jump rate between the triplet of equivalent electronic Jahn-Teller distortion directions measured by EPR (Ref. 2) for V_2^- is many orders of magnitude higher than the rate of electron emission from the traps at $E_c-0.23$ and $E_c-0.42$ eV. Thus these levels are attributed to the motionally averaged state and not to the low-symmetry C_{2h} configuration where the divacancy is frozen in low-temperature EPR and IR measurements.

II. EXPERIMENT

P^+-n diodes were fabricated using high-purity neutron transmutation doped silicon with a donor concentration of 3×10^{13} or 1.1×10^{14} cm^{-3} as starting material. The wafers were grown in the ⟨111⟩ direction. Firstly, in order to ensure a low series resistance the backsides of the wafers were implanted with a high dose of phosphorus ions. The p^+ regions were then accomplished by implantation of 40-keV boron ions to a dose of 5×10^{14} cm^{-2} and a subsequent thermal annealing at 1000 °C for 1 h yielding a junction depth of ~ 0.8 μm. Frontside and backside contacts were formed by the deposition of aluminum in a high vacuum evaporator followed by a heat treatment at 400 °C for 30 min in an argon ambient.

The wafers were cut into separate diodes, and those fabricated in the high-resistivity material were irradiated with 1.3-MeV protons or 5.0-MeV α particles while the others were bombarded with ions of $^{16}O^{4+}$, $^{32}S^{7+}$, $^{79}Br^{8+}$, or $^{127}I^{10+}$ using energies of 16, 33, 46, or 50 MeV, respectively. The irradiations were performed at the tandem accelerator at The Svedberg Laboratory utilizing a sample chamber designed for accurate and uniform low dose bombardments.[16] The experiments were carried out at nominal room temperature using dose rates of $\sim 10^7$–10^8 cm^{-2}s^{-1} and doses in the range of 1×10^7 to 1×10^{10} cm^{-2}.

The irradiated diodes were mounted in TO5 headers in order to undertake the DLTS measurements. The DLTS setup has been described in detail elsewhere.[17] The sample temperature was scanned between 80 and 280 K, and the registrated capacitance transients were averaged within intervals of a width of 1.0 K. The DLTS signal was extracted from the transients applying a lock-in type of weighting function, and eight traditional DLTS spectra with rate windows in the range of (20 ms)$^{-1}$ to (2.56 s)$^{-1}$ were obtained from a single temperature scan. Concentration, energy level position, and capture cross section were subsequently evaluated from the spectra stored in the computer memory. During all the measurements the diodes were reversed biased, and no forward bias injection of minority carriers was performed.

Depth concentration profiles were determined by keeping the steady state reverse bias voltage constant while gradually increasing the amplitude of the majority carrier pulse. The sample temperature was held constant within ±0.25 K at the maximum of the studied peak, and only one single rate window was utilized. The depth profiles were then extracted from the dependence of the DLTS signal on the pulse amplitude.[12]

III. RESULTS

In Fig. 1 DLTS spectra from samples irradiated with electrons (2 MeV) and ions of helium, oxygen, and bromine are displayed. Two major peaks appear ~ 0.23 and

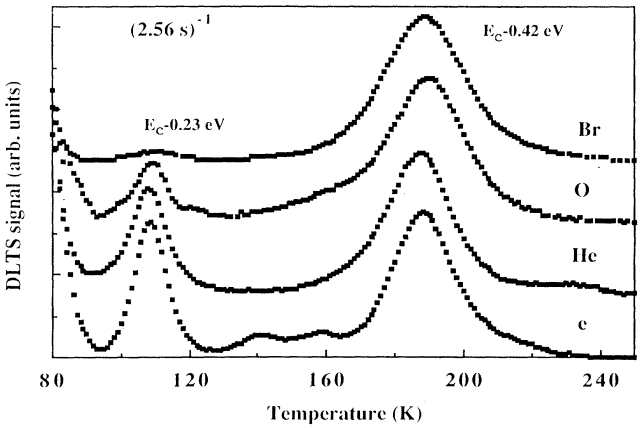

FIG. 1. DLTS spectra from *n*-type silicon samples irradiated with electrons (2 MeV, 3×10^{15} cm^{-2}) and ions of $^4He^{2+}$ (5 MeV, 5×10^8 cm^{-2}), $^{16}O^{4+}$ (16 MeV, 1×10^8 cm^{-2}) and $^{79}Br^{8+}$ (46 MeV, 2×10^7 cm^{-2}). [Rate window (2.56 s)$^{-1}$.]

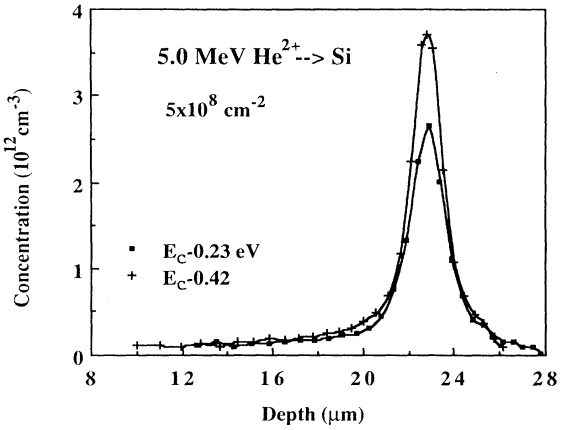

FIG. 3. Depth concentration profiles of the levels at $E_c-0.42$ eV and $E_c-0.23$ eV in a sample bombarded with 5-MeV α particles to a dose of 5×10^8 cm^{-2}.

$\sim$0.42 eV below E_c, and the corresponding capture cross sections are both approximately 2×10^{-15} cm^2. The spectra indicate also a third peak at low temperatures which is not fully resolved above 80 K using a rate window of (2.56 s)$^{-1}$; results for shorter windows yield a position of $\sim E_c-0.17$ eV with a capture cross section of $\sim2\times10^{-14}$ cm^2. This latter trap originates from the well-known vacancy-oxygen center and has been extensively studied by numerous authors; see, for example, Ref. 13. In the following, we will concentrate on the first two levels which are of acceptor type and attributed to the doubly and singly negative charge states of V_2, respectively. In the electron-irradiated sample the amplitudes of the two peaks are essentially identical while for the heavier projectiles the ratio $[E_c-0.42\text{ eV}]/[E_c-0.23\text{ eV}]$ increases gradually with increasing ion mass. For ^{79}Br ions $[E_c-0.42\text{ eV}]$ is more than one order of magnitude higher than $[E_c-0.23\text{ eV}]$.

Figure 2 shows the peak amplitude of the level at $E_c-0.42$ eV for different pulse voltages versus that of $E_c-0.23$ eV using results from four different samples irradiated with 2.0-MeV electrons and doses in the range of $1-3\times10^{15}$ cm^{-2}. As reported previously,[12] a close one-to-one proportionality holds, and the depth concentration profiles of the two levels are identical.

Depth profiles observed in a sample bombarded with 5×10^8 (α particles)/cm^2 are depicted in Fig. 3, and $[E_c-0.42\text{ eV}]$ is about 50% higher than $[E_c-0.23\text{ eV}]$ in the peak region while they are almost identical in the tail towards the surface. Figure 4 compares the strengths of the two levels in proton-bombarded samples for different pulse amplitudes while keeping the steady state reverse bias voltage constant at -15 V. The corresponding depth interval is $\sim18-26$ μm and includes the damage peak. $[E_c-0.42\text{ eV}]$ increases more strongly with the pulse amplitude than $[E_c-0.23\text{ eV}]$, and large deviations

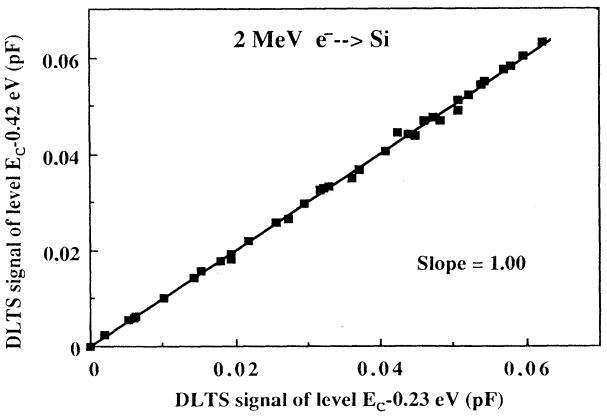

FIG. 2. The amplitude of the DLTS signal of level $E_c-0.42$ eV obtained at different pulse voltages vs that of level $E_c-0.23$ eV. Results from four different samples irradiated with electrons to doses in the range of $1-3\times10^{15}$ cm^{-2} are included.

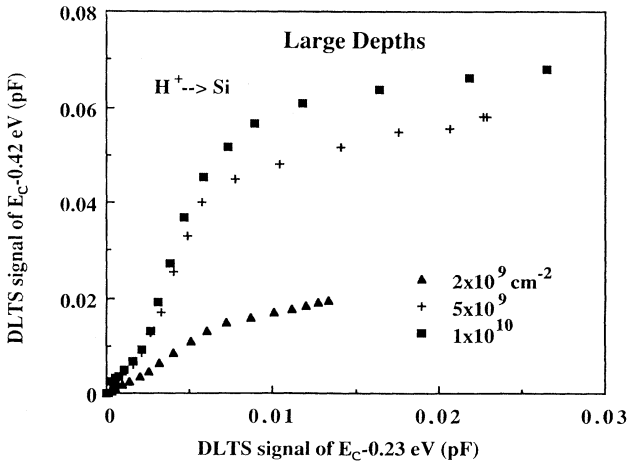

FIG. 4. The amplitude of the DLTS signal of level $E_c-0.42$ eV obtained at different pulse voltages vs that of level $E_c-0.23$ eV in samples irradiated with different doses of protons. The voltages correspond to a depth interval of $\sim18-26$ μm.

TABLE. I. Dose dependence of the ratio between the DLTS signals of the levels at $E_c-0.42$ eV and $E_c-0.23$ eV, $S_{0.42}/S_{0.23}$, for protons and α particles. Values are given for both shallow ($\sim 8-16$ μm) and deep ($\sim 18-26$ μm) depth intervals.

Ion	Dose (cm^{-2})	$S_{0.42}/S_{0.23}$ shallow region	$S_{0.42}/S_{0.23}$ deep region
$^1H^+$	2×10^9	1.04	1.48
	5×10^9	0.99	2.53
	1×10^{10}	0.97	2.57
$^4He^{2+}$	5×10^8	1.03	1.36
	1×10^9	0.96	1.47

from a one-to-one proportionality are found. These deviations increase with ion dose, and values of the ratio between the amplitudes of the two DLTS signals are given in Table I for different doses of protons and α particles. Figure 5 presents a plot similar to Fig. 4 but for shallow depths ($\sim 8-16$ μm), and a least-squares fit reveals a slope of 1.00 with a correlation coefficient higher than 0.99. This holds for both protons and α particles using doses in the range of $5\times10^8-1\times10^{10}$ cm^{-2}; see also Table I.

IV. DISCUSSION AND CONCLUSIONS

A. Depth profiles

In electron-irradiated samples the depth concentration profiles of the levels at $E_c-0.23$ and $E_c-0.42$ eV are identical, and moreover, a close correlation between their production rates as a function of bombardment energy as well as between their annealing kinetics was reported by Evwaraye and Sun.[11] The collected data provide almost conclusive evidence for the interpretation that the two levels correspond to different charge-state transitions of V_2, presumably $(2-/-)$ and $(-/0)$, respectively. However, if the complete depth profiles in ion-irradiated samples are monitored large deviations from a one-to-one correlation are observed while a strong proportionality holds at depths shallower than the damage peak region. Thus in a lattice accommodating a high enough density of damage [$E_c-0.23$ eV] is reduced relative to [$E_c-0.42$ eV] and disappears almost totally for heavy ion bombardment. It may also be pointed out that the relative loss of [$E_c-0.23$ eV] is not due to a Fermi level effect. The defect concentrations were typically at least one order of magnitude smaller than the dopant concentration, and the DLTS spectra in Fig. 1 indicate a Fermi level position which is high enough to populate the vacancy-oxygen acceptor level at $E_c-0.17$ eV.

In this context it appears appropriate to emphasize the large difference between defect formation by MeV electron irradiation and by MeV ion irradiation. In the first case, a uniform distribution of highly isolated point defects over depths of several millimeters is generated while in the latter case a nonuniform depth distribution with a peak in the range of $\sim 5-30$ μm is obtained. For protons the generation rate of defects by elastic collisions is at least 3 to 4 orders of magnitude larger than that for electrons. Recent results by Holland *et al.*[18] for MeV ion implantation in silicon revealed two distinct regions for damage nucleation; one in the near-surface region where damage accumulation saturates and "simple" point defects dominate and one at the end of the ion range where more stable and extended defects are formed. These latter defects subsequently give rise to a continuous amorphous layer at high enough doses.

The ratio [$E_c-0.42$ eV]/[$E_c-0.23$ eV] increases with the accumulated damage density as illustrated by the dose dependence, but it hinges also strongly on the rate of elastic energy deposition per projectile (generated vacancies per Å and projectile). This can be seen by a comparison of the DLTS curves for α particles and oxygen ions

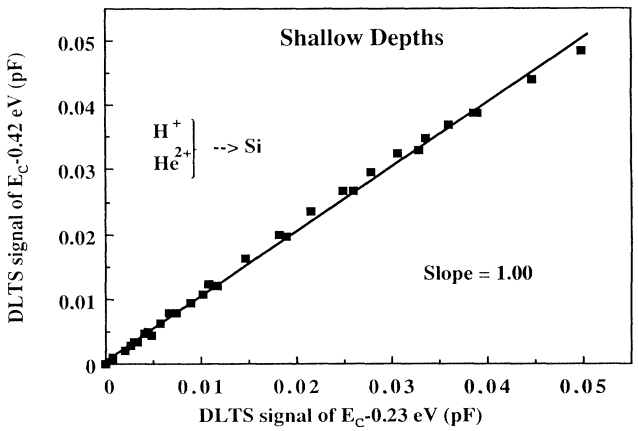

FIG. 5. The amplitude of the DLTS signal of level $E_c-0.42$ eV obtained at different pulse voltages vs that of level $E_c-0.23$ eV in samples irradiated with different doses of protons and α particles, $2\times10^9-1\times10^{10}$ cm^{-2} and $5\times10^8-1\times10^9$ cm^{-2}, respectively. The voltages correspond to a depth interval of $\sim 8-16$ μm.

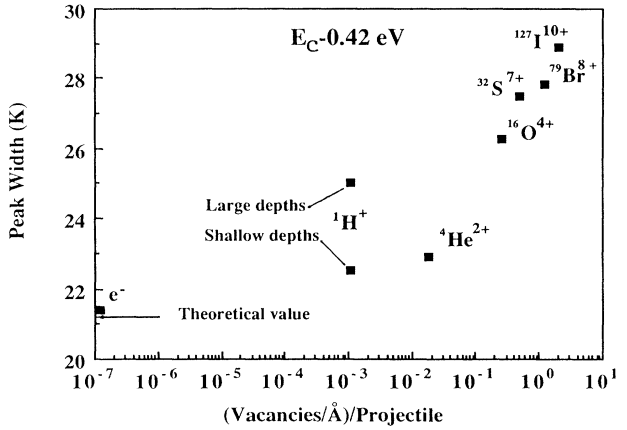

FIG. 6. The full width at half maximum of the level at $E_c-0.42$ eV using a rate window of $(2.56\ s)^{-1}$ vs the number of generated vacancies per Å and projectile for 2-MeV electrons, 1.3-MeV protons, 5-MeV α particles, 16-MeV $^{16}O^{4+}$ ions, 33-MeV $^{32}S^{7+}$ ions, 46-MeV $^{79}Br^{8+}$ ions, and 50-MeV $^{127}I^{10+}$ ions.

in Fig. 1. The two curves correspond approximately to the same amount of deposited energy while the deposition rate per ion is more than one order of magnitude higher for oxygen. The $^{16}O^{4+}$ ions generate more complex (higher-order) defects than the $^{4}He^{2+}$ ions since the collision cascades have a larger density; the damaged regions are more localized, and individual heavy ions may even produce localized amorphous zones.[19] Thus V_2 centers formed by heavy ion bombardment occur in lattice regions which accommodate a larger strain than that for light ion bombardment, and as a result, the relative strength of $[E_c-0.23$ eV] decreases.

Furthermore, the type of projectile influences also the width of the $E_c-0.42$ eV peak, and a broadening towards low temperatures with increasing projectile mass is observed, Fig. 6. The numbers of generated vacancies per Å and projectile given in Fig. 6 correspond to the damage peak maximum for each ion and are estimated using Monte Carlo simulations applying the transport of ions in matter code (TRIM, versions 87 and 89) originally developed by Biersack and Haggmark.[20] Overlap from the E-center level[21] $[E_c-0.45$ eV] is expected to play only a minor role: the E centers are stable up to temperatures of ~ 150 °C, and spectra from samples annealed at 150 °C for 30 min revealed no reduction of the peak width. The broadening reflects presumably a lattice with gradually increasing distortion and concurrently, the relative strength of $[E_c-0.23$ eV] decreases and ultimately, also the V_2^- peak will be smeared out. Measurements of the complete capacitance transient of the V_2^- peak as a function of time at a constant temperature showed an exponential decay; the increase of the peak width is interpreted as a shift of the initially well-defined level originating from an unperturbed V_2 complex and is not caused by a nonexponential capacitance transient.

For protons a substantially larger width of the V_2^- peak than expected from the generation rate of vacancies/Å was obtained at large depths while a more ordinary value was extracted at shallow depths. For α particles no such effect was observed. Hydrogen is known to interact strongly with defects in silicon, and it is generally agreed that the lowest-energy state for hydrogen is bonded to a dangling bond of a vacancy-type defect.[22] The large peak width is attributed to an increase of the lattice strain around the V_2 centers because of implanted hydrogen atoms trapped in the damage peak region. According to TRIM simulations the peak of the hydrogen implantation profile is shifted ~ 1 μm towards large depths compared with that for the elastic energy deposition profile, and it exhibits also a significantly smaller skewness towards the surface. The hydrogen atoms are, therefore, predominantly trapped at large depths close to the damage peak, and only a minor influence is expected at shallow depths.[23]

B. Origin of the $E_c-0.23$ eV and $E_c-0.42$ eV levels

The lack of a one-to-one correspondence between $[E_c-0.23$ eV] and $[E_c-0.42$ eV] in regions with a high density of damage shows that the shallow level is more affected by the lattice strain, and at least two models for the singly and doubly negative charge states can be put forward.

(I) Lindefelt and Wang[24] proposed recently the existence of two different configurations of the V_2^{2-} charge state. Utilizing the linear combination of atomic orbitals (LCAO) model normally applied for the V_2 center,[2] they deduced not only one "ordinary" V_2^{2-} configuration corresponding to a fully occupied gap level (e_u) and consequently a totally symmetric charge density with respect to the point group D_{3d} but also one originating from adding one electron to the a_{1g}-symmetric level of the Jahn-Teller distorted charge state V_2^- (point group C_{2h}). On the basis of the Hellmann-Feynman theorem it was argued that the latter process would not give rise to a symmetry-breaking force with respect to the group C_{2h} since the resulting charge density after capture is totally symmetric. Thus it was concluded that both the configurations $V_2^{2-}(D_{3d})$ and $V_2^{2-}(C_{2h})$ exist in principle, and the latter is likely to be lowest in energy. In order to account for the proportionality between $[E_c-0.23$ eV] and $[E_c-0.42$ eV] at shallow depths and in electron-irradiated samples both levels are attributed to the C_{2h} symmetry configuration. However, under this assumption it seems difficult to explain why the EPR $G7$ spectrum (originating from V_2^-) appears although the Fermi level is above $E_c-0.23$ eV. This contradiction as well as other observations made by EPR, electron-nuclear double resonance, photoconductivity, and IR absorption have to be fully resolved in order to verify the validity of the model.

(II) According to EPR measurements V_2^+ and V_2^- exhibit motional effects; electronic bond switching between the triplet of equivalent distortion directions corresponding to the C_{2h} symmetry occurs. Ultimately, the jump rate becomes so high that the defect does not relax in the low-symmetry configurations, and a motionally averaged state with an effective D_{3d} symmetry appears.[2,9,10] This electron reorientation process is thermally activated, and on the basis of linewidth and stress studies the following relation was determined by Watkins and Corbett[2] for the jump rate of V_2^- in s^{-1}:

$$1/\tau_{re}=1.1\times 10^{13}\exp[-0.056\ (\text{eV})/kT]$$

where k is Boltzmann's constant and T is the absolute temperature. At 110 K $1/\tau_{re}\sim 10^{10}$ s^{-1} while the rate of electron emission, $1/\tau_{em}$, from the level at $E_c-0.23$ eV is ~ 1 s^{-1}. For the trap at $E_c-0.42$ eV $1/\tau_{em}$ is ~ 1 s^{-1} at 190 K with a corresponding $1/\tau_{re}$ of $\sim 3\times 10^{11}$ s^{-1}. Hence at the temperatures where the DLTS measurements are performed $\tau_{re}\ll\tau_{em}$, and an assignment of the two levels with the motionally averaged state appears highly appropriate. The averaged state of V_2^- shows a good agreement with the LCAO picture,[10] and the $E_c-0.23$ eV level should correspond to the position of the fully occupied e_u orbital while the $E_c-0.42$ eV level represents the e_u orbital partially filled with three electrons. At low enough temperatures the thermal energy is not sufficient in comparison with the barrier for reorientation, and V_2^- is frozen in a distorted C_{2h} symmetry

configuration. Consequently, the e_u orbital splits and the positions of the charge-state transitions in the band gap change; in particular, the $E_c-0.23$ eV level does not exist at the low temperatures (≤ 20 K) where IR absorption and EPR measurements of V_2^- are normally performed. The position of the $V_2(-/0)$ level in the distorted configuration (corresponding to the a_{1g} defect orbital) is estimated to be between 0.41 and 0.48 eV below E_c while the capture of the second acceptor electron with an accompanying reorientation to D_{3d} symmetry for V_2^{2-} presumably occurs to a shallow state in the range of ~ 0.07 to 0.13 eV below E_c.[8]

EPR studies undertaken at 30 K have shown that the direction of the Jahn-Teller distortion of the V_2^- and V_2^+ centers can be preferentially aligned by applying uniaxial stress, and the importance of motional averaging diminishes,[2] i.e., the centers are "locked" and the jump rate for reorientation decreases substantially under the presence of stress. Thus the internal lattice strain associated with the damage peak region in ion-irradiated samples prevents, to a large extent, reorientation, and since the reorientation is a thermally activated process these effects are most dominant at low temperatures. The peak at $E_c-0.23$ eV is, therefore, more affected than that at $E_c-0.42$ eV, and as a result, the close one-to-one proportionality between $[E_c-0.23$ eV$]$ and $[E_c-0.42$ eV$]$ breaks down. Furthermore, the second acceptor electron is less localized than the first electron because of the lower binding energy and is expected to be more influenced by the distorted atomic positions in a strained lattice.

Finally, in the averaged state the acceptor electrons are captured to a rather delocalized six-silicon-atom complex with an effective symmetry of D_{3d}. An analogy with a highly localized double negative center showing strong electron-electron interaction is not valid, and the capture cross sections of the two transitions $V_2(2-/0)$ and $V_2(2-/-)$ may not differ by several orders of magnitude.

V. SUMMARY

The depth profiles of the two V_2-related acceptor levels at $E_c-0.23$ eV and $E_c-0.42$ eV, respectively, have been studied in detail for ion-bombarded specimens. The concentrations of the two levels are identical in the tail towards the surface while $[E_c-0.23$ eV$]$ is significantly lower than $[E_c-0.42$ eV$]$ in the damage peak region. The ratio $[E_c-0.42$ eV$]/[E_c-0.23$ eV$]$ increases with bombardment dose and also with the energy deposited per ion and unit length into elastic collisions. Furthermore, the rate of elastic energy deposition influences also the width of the $E_c-0.42$ eV peak, and a broadening towards low temperatures with increasing projectile mass is observed. For heavy ions the rate of energy deposition is higher and more complex defects are generated; the V_2 centers occur in lattice regions which accommodate a large strain, and as a result, the initially well-defined level at $E_c-0.42$ eV originating from an unperturbed V_2 complex is broadened. Concurrently, the relative strength of $[E_c-0.23$ eV$]$ is dramatically reduced, and ultimately, this level may disappear totally.

Evidence for a new model where the two levels are attributed to motionally averaged states of V_2^{2-} and V_2^-, respectively, is put forward. The model explains several of the major properties of the V_2 center observed experimentally by different techniques and must be regarded as a promising candidate for future exploitation and more conclusive tests. One key issue concerns a comprehensive theoretical treatment of the motionally averaged states with their associated molecular orbitals and energy levels. Several defects are suspected to have a similar kind of averaged states, e.g., the monovacancy[25] and the E center,[26] and the establishment of electronic energy levels related to dynamic states may not only be limited to the divacancy but also include other defects.

ACKNOWLEDGMENTS

Financial support was partially received from the Swedish Board for Technical Development, the Swedish Natural Science Research Council, the U.S. Solar Energy Research Institute, and the Mobil Foundation.

[1]J. W. Corbett and G. D. Watkins, Phys. Rev. Lett. **7**, 314 (1961).
[2]G. D. Watkins and J. W. Corbett, Phys. Rev. **138**, A543 (1965).
[3]A. H. Kalma and J. C. Corelli, Phys. Rev **173**, 734 (1968).
[4]R. C. Young and J. C. Corelli, Phys. Rev. B **5**, 1455 (1972).
[5]L. J. Cheng, J. C. Corelli, J. W. Corbett, and G. D. Watkins, Phys. Rev. **152**, 761 (1966).
[6]L. J. Cheng and P. Vadja, Phys. Rev. **186**, B816 (1969).
[7]F. Carton-Merlet, B. Pajot, D. T. Don, C. Porte, B. Clearjaud, and P. M. Mooney, J. Phys. C **15**, 2239 (1982).
[8]J. H. Svensson, B. G. Svensson, and B. Monemar, Phys. Rev. B **38**, 4192 (1988).
[9]J. G. deWit, E. G. Sieverts, and C. A. J. Ammerlaan, Phys. Rev. B **14**, 3494 (1976).
[10]E. G. Sieverts, S. H. Muller, and C. A. J. Ammerlaan, Phys. Rev. B **18**, 6834 (1978).
[11]A. O. Evwaraye and E. Sun, J. Appl. Phys. **47**, 3776 (1976).
[12]B. G. Svensson and M. Willander, J. Appl. Phys. **62**, 2758 (1987).
[13]L. C. Kimerling, in *Radiation Effects in Semiconductors 1976,* Inst. Phys. Conf. Ser. No. 31, edited by N. B. Urli and J. W. Corbett (IOP, Bristol, 1977), p. 221.
[14]E. G. Sieverts, S. H. Muller, and C. A. J. Ammerlaan, Solid State Commun. **28**, 221 (1978).
[15]A. Hallén, B. U. R. Sundqvist, Z. Paska, B. G. Svensson, M. Rosling, and J. Tirén, J. Appl. Phys. **67**, 1266 (1990).
[16]A. Hallén, P. A. Ingemarsson, P. Håkansson, G. Possnert, and B. U. R. Sundqvist, Nucl. Instrum. Methods B **36**, 345 (1989).

[17]B. G. Svensson, K.-H. Rydén, and B. M. S. Lewerentz, J. Appl. Phys. **66**, 1699 (1989).
[18]O. W. Holland, M. K. El-Ghor, and C. W. White, Appl. Phys. Lett. **53**, 1282 (1988).
[19]L. M. Howe and M. H. Rainville, Nucl. Instrum. Methods **182/183**, 143 (1981).
[20]J. P. Biersack and L. G. Haggmark, Nucl. Instrum Methods **174**, 257 (1980).
[21]G. D. Watkins, J. W. Corbett, and R. M. Walker, J. Appl. Phys. **30**, 1198 (1959).
[22]J. W. Corbett, J. L. Lindström, and S. J. Pearton, MRS Symp. Proc. **104**, 229 (1988), and references therein.
[23]B. G. Svensson, A. Hallén, and B. U. R. Sundqvist, J. Mater. Sci. Eng. B **4**, 285 (1989).
[24]U. Lindefelt, and Wang Yong-Liang, Phys. Rev. B **38**, 4107 (1988).
[25]G. D. Watkins, J. Phys. Soc. Jpn. **18**, 21 (1963).
[26]G. D. Watkins and J. W. Corbett, Phys. Rev. **134**, A1359 (1964).